2014 IEEE International Conference on Robotics & Automation (ICRA)
Hong Kong Convention and Exhibition Center
May 31 - June 7, 2014. Hong Kong, China

Simple Passive Valves for Addressable Pneumatic Actuation

Nils Napp*, Brandon Araki+, Michael T. Tolley*, Radhika Nagpal*, Robert J. Wood*
{nnapp@wyss, mike.tolley@wyss, rad@eecs, rjwood@seas}.harvard.edu brandon.araki@yale.edu
*Wyss Institute
Harvard University
Cambridge MA, USA
+Yale University
New Haven CT, USA

***Abstract*— We present a method for setting the pressure of multiple chambers using a single pressure source when they are interconnected via *band-pass valves*. These valves can be constructed from simple passive devices that behave like leaky check valves. We present the theory of operation and design parameters for individual valves, give a control strategy for serial connections of pressure chambers, and demonstrate the approach by building prototype valves and using them to control serially connected soft-robotic actuators from a single pressure source.**

I. Introduction

A. Motivation

Developing novel soft robots that use pneumatic or hydraulic actuation to achieve complicated compliant motion is currently an active area of research [1], [2], [3], [4]. Soft robots can be very inexpensive to manufacture while being robust to harsh chemical and physical environments that are extremely challenging for existing robots [5]. The compliant structure of soft robots also allows novel motion and grasping strategies that are difficult to implement with rigid parts. Instead of motors and gears, these robots use integrated, distributed actuators to control their infinite degrees of freedom. One successful approach is to actuate pneumatic channels in flexible bodies with pressurized air [6].

Typically, these designs employ solenoid valves to control the flow of the working fluid into and out of the actuators. While solenoid valves are readily available and simple to control, they have three principal drawbacks for flow control in soft robots: they are composed of rigid, electromagnetic components; they are relatively expensive and are often the most expensive component in systems with many actuators; and their miniaturization is limited by the disadvantageous scaling of electromagnetic forces at small scales [7].

We describe a simple passive valve design that behaves like a leaky check valve and can be used to control the pressures in a network of multiple connected chambers from a single input. The simple mechanical design of these valves could allow them to be integrated into current elastomeric manufacturing techniques for soft robots and potentially miniaturized for other applications. The central concept is to exchange lower valve complexity for greater complexity of the pressure source. Through deliberate modulation of the system's input pressure, the passive valves throughout the system can be selectively opened and closed to fill and drain pressure chambers. For soft robots, this means that logic and control can be baked into the mechanism itself. For example, a soft-robotic tentacle with multiple chambers (e.g. [8]) incorporating these types of valves could achieve many poses using only a single external connection while at the same time making the overall robot less expensive and more mechanically robust.

The contribution of this paper is to present a device design and associated control strategy for making this tradeoff. The control strategy described in Sec. II is developed for an idealized behavior of the valve. We present a particular valve implementation for use with soft robots in Sec. III and demonstrate the configuration of multiple soft-robotic actuators from a single pressure source Sec. IV.

B. Related Work

A majority of the previous work on pneumatically actuated soft robotics has used off-board or on-board solenoid valves to control the flow of pressurized air to the actuators [8], [9], [6], [5]. However, solenoid valves have the disadvantages mentioned above of being difficult to integrate, expensive, and difficult to miniaturize. Marchese et al. investigated the use of electropermanent magnets to create energy-efficient valves for soft robots that only consume energy while switching between open and closed states [10]; However, aside from their efficiency these valves have similar challenges as solenoid valves, since they also employ electromagnets.

Related previous work has also used passive valves for actuating robots. Nishioka et al. demonstrated passive valves that can be activated by acoustic waves through the working fluid [11]. However, while passive, their valves require resonant mechanical structures that may be difficult to integrate into current manufacturing techniques for soft robots. Shepherd et al. used passive soft valves molded into the body of soft robots that used internal explosions for rapid actuation [12]. Similar to the valves presented here, these passive valves remained open at low pressures differentials (to allow the venting of combustion products) but closed during the rapid pressure increase caused by the explosions. However, these valves were not designed or characterized to achieve hold states or to be individually addressable, and off-board solenoid valves and spark ignition electronics were required to control actuation.

Small-scale soft valves are also an active area of research in microfluidics[13], where they are used for the control of fluid flow on chips through channels with dimensions of tens of micrometers. A common approach in microfluidics is the use of a secondary pressurized pneumatic layer to valve a primary fluidic layer [14]. While this approach significantly reduces the complexity of the microfluidic chips, each independently addressable pneumatic valve is still controlled off-board by a solenoid valve, effectively maintaining the cost and complexity of the overall system. Recent work has sought to remedy this problem by developing latching valves to achieve on-board digital control logic for multiplexing

978-1-4799-3684-7/14/$31.00 ©2014 IEEE

valves [15], [16], [17]. However, devices of this sort have not been demonstrated that can achieve the pressures and flow rates required to valve soft robots.

II. Valve Design and Theory of Operation

The idea is to design a passive valve that allows pressurizing several chambers to different levels, i.e. *pressure configurations*, using a single modulated pressure source. The particular approach described here is a valve that behaves like a leaky check valve that always allows flow in the forward direction, but only allows a certain amount of backward flow before closing. Physically, this can be implemented by a introducing a small gap in a regular check valve design. Connecting two of these valves in series creates a ***band-pass valve*** that only allows low flow rates. When these band-pass valves are used to connect several pressure chambers, a single modulated pressure source can be used to reach arbitrary pressure configurations by selectively closing some valves while feeding pressure chambers through the open ones.

A. Device Model and Control Strategy

This section describes the idealized behavior of a leaky check valve where the maximum leaking rate can be carefully controlled. The symbol to represent the device and the desired operational behavior are shown in Fig. 1(a) and Fig. 1(b). The forward flow through the valve is proportional to the pressure difference across the device. In the backward direction, the flow through the valve is also proportional to the pressure difference up to a critical value called the ***shutoff pressure***, $\Delta P_{\text{shutoff}}$, beyond which the valve closes and prevents flow. Thus, the volumetric flow through the device, $\dot{V}$, is related to the pressure differential across the device ΔP, and flow resistance R in the following way:

$$\dot{V} = \begin{cases} \frac{\Delta P}{R} & , -\Delta P_{\text{shutoff}} < \Delta P \\ 0 & , \text{otherwise.} \end{cases} \quad (1)$$

The maximal leaking rate is given by $\dot{V}_{\text{shutoff}} = -\frac{\Delta P_{\text{shutoff}}}{R}$. Using a single such valve connected to the input of a pressure chamber allows the chamber to be both inflated and deflated using a single pressure source. Just like a regular check valve, the chamber can be inflated and the pressure source removed. However, unlike a regular check valve the same pressure source can be used to deflate the pressure chamber by keeping the pressure source below, but within $\Delta P_{\text{shutoff}}$, of the chamber pressure.

Two of these devices can be connected into a ***band-pass valve*** configuration shown Fig. 1(c). Each individual valve can stop flow through both of them, and since they face in opposite directions, this combined device now has a shutoff pressure in both directions, Fig. 1(d). The result is a device that allows low flow in both directions, but shuts off at high flows in either direction. Although there is no such restriction in practice, the following discussion assumes that the shutoff pressures are symmetric for simplicity. The idealized behavior of this band-pass valve is characterized by the pressure and flow ***pass-band***, which are given by $\Delta P_{\text{shutoff}} < |\Delta P|$ and $\dot{V} < |\dot{V}_{\text{shutoff}}|$ respectively.

When this band-pass valve is used to connect two pressure chambers in series, Fig.1(e), a single modulated pressure source, P_{in}, can be used to pressurize both chambers to different levels. When $P_1 > P_2 + \Delta P_{\text{shutoff}}$ one of the valves is closed and prevents flow that would otherwise equalize the two chambers, and when $P_2 > P_1 + \Delta P_{\text{shutoff}}$ the other valve is closed. All pressure combinations where $|P_1 - P_2| > \Delta P_{\text{shutoff}}$ or $P_1 = P_2$ are thus stable configurations with this arrangement, Fig. 1(f).

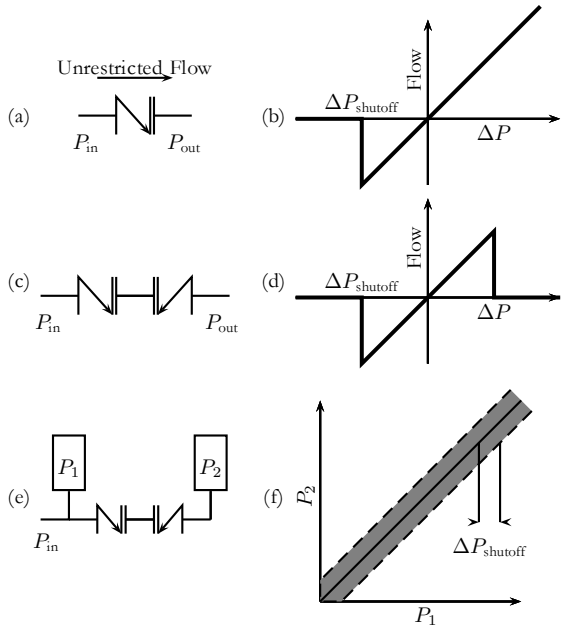

Fig. 1. (a) Valve Diagram showing pressure ports and flow direction. The pressure across the valve is $\Delta P = P_{out} - P_{in}$. (b) Schematic of idealized pressure vs. flow profile, showing the shutoff pressure in one direction and unimpeded flow in the other. (c) Diagram of two valve band-pass configuration. (d) Idealized pressure vs. flow profile for band-pass valve. Pressures below the shutoff pressures result in normal flow. Pressure differentials outside the pass-band close one of the valves and result in zero flow. (e) Diagram of two pressure chambers connected via a band-pass valve. (f) Reachable stable pressures in the configuration space. The gray area around the diagonal is excluded. Configurations in this range do not cause either valve to close, so the two chambers equilibrate to $P_1 = P_2$.

B. Control Strategy

The space of pressure configurations for N pressure chambers is $P^N = \mathbb{R}^N_{>0}$, the N-fold cross product of the non-negative real numbers. In this section we describe a strategy for reaching all stable configurations when the pressure chambers are arranged in series and connected via $N-1$ band-pass valves with decreasingly nested flow pass-bands, and a modulated pressure source, P_{in}, is connected to the first chamber with pressure P_1, e.g. Fig. 1(e).

The shutoff flow rate for the pass-band valve connecting pressure chamber i and $i+1$ is given by $\dot{V}^i_{\text{shutoff}} = \frac{\Delta P^i_{\text{shutoff}}}{R^i}$ and the following scheme requires that $V^i_{\text{shutoff}} > V^{i+1}_{\text{shutoff}}$ by some sufficiently large margin so valve i can be closed without closing any of the valves $j < i$. The required amount of separation depends the actuation fidelity of the source, the precision of valve characteristics, and on the nature of the pressure chambers: large and expandable chambers require more separation, see Sec. II-B.1 for details.

The control strategy has two steps, first a strategy to reach an arbitrary stable configuration when initially none of the valves are closed, and second, a strategy for going from an arbitrary configuration to one where all the pressures in all chambers are equal and all valves are open.

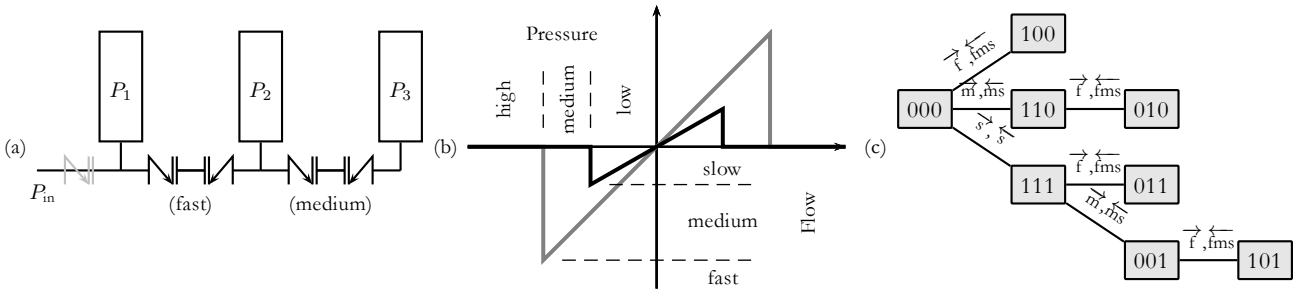

Fig. 2. (a) Schematic of three chambers in series connected via band-pass valves. The experimental setup described in Sec. IV includes the gray valve at the input to allow the pressure source to be disconnected. (b) Flow vs. pressure profile of the two band-pass valves with labeled pressure regions that induce f(ast), m(edium), and s(low) flows. (c) Binary configuration tree. From a given configuration, different actions can result in different transitions. The edges are labeled where the overhead arrow indicates the direction. Each transitions changes the least significant bit (LSB, left) and wether a transition corresponds to pressurizing or depressurizing chambers depends on wether the LSB changes from 0 to 1 (pressurizing) or from 1 to 0 (depressurizing).

The strategy for reaching a particular stable target configuration $P^* \in P^N$ is to iteratively pressurize chambers, starting with P_N, i.e. the chamber that is furthest from the pressure source. The pressure is modulated to slowly pressurize all chambers to the target pressure P_N^* of the last chamber. Then, depending on whether P_{N-1}^* is larger or smaller than P_N^*, the modulated pressure source increases (or decreases) quickly enough to close the last band-pass valve between chambers $N-1$ and N and to pressurize the first $N-1$ chambers to the target pressure P_{N-1}^*. When the target pressure is reached, the pressure is changed quickly enough to close the valve between chambers $N-2$ and $N-1$, and to adjust the pressure of the first $N-2$ chambers to P_{N-2}^*, etc. These serially connected chambers act like a shift register for pressures.

Given an arbitrary stable pressure configuration, reaching a state where all valves are open can be achieved by reversing the above process. First P_1 is adjusted to $P_2 \pm \Delta P^1_{\text{shutoff}}$ and the two chambers are allowed to equilibrate. Then the first two chambers are brought to the level of $P_3 \pm \Delta P^2_{\text{shutoff}}$ and allowed to equilibrate, etc. until all the chambers are at the same pressure and none of the valves are closed. Finally, the pressure of all chambers can be adjusted simultaneously to some desired level, e.g. ambient pressure.

1) Separation of Pass-Bands: In this serial configuration, the flow coming out of a valve splits into flow that fills the pressure chamber and flow that goes into the downstream valve. To describe how the flow splits we define the fill resistance R^i_{fill} of chamber i to be the resistance to volumetric flow for changing the chamber pressure. By ignoring any flow resistance from the input port, differentiating the ideal gas law ($P_iV_i = n\bar{R}T$) in terms of time, and setting $\dot{n} = \frac{P_i\dot{V}_{\text{in}}}{\bar{R}T}$ the fill resistance is found to be

$$R^i_{\text{fill}} = \frac{1}{\frac{V_i}{P_i} + \frac{\partial V_i}{\partial P_i}}. \tag{2}$$

A chamber that has either a large volume V_i or that expands easily, i.e. $\frac{\partial V_i}{\partial P_i}$ is large, has a low resistance to volumetric flow that is diverted to change the pressure inside the chamber. Assuming equal pressures in chamber i and upstream chambers, the flow $\dot{V}^{i-1}$ coming into chamber i splits so that the flow $\dot{V}^i$ going into the next valve is given by

$$\dot{V}^i = \frac{R^i_{\text{fill}}}{{R_{\text{fill}}}^i + R^i}\dot{V}^{i-1}. \tag{3}$$

If the fill resistance is large ,then the flows in and out of the chamber are approximately equal. When the fill resistance is low, as is the case in soft robots with large expandable chambers, then the pass-bands in the series connection need to be separated by

$$\dot{V}^i_{\text{shutoff}} < \frac{R^i_{\text{fill}}}{R^i_{\text{fill}} + R^i}\dot{V}^{i-1}_{\text{shutoff}}. \tag{4}$$

This restriction allows the i-th valve to be closed without closing any of downstream valves $j < i$.

Equivalently, the relation can be stated as a requirement on shutoff pressures

$$\Delta P^i_{\text{shutoff}} < \frac{R_i}{R_{i-1}} \quad \frac{R^i_{\text{fill}}}{R^i_{\text{fill}} + R^i}\Delta P^{i-1}_{\text{shutoff}}. \tag{5}$$

This representation highlights the fact that it is good for upstream valves to have a low flow resistance compared to downstream valves. By allowing more flow at similar pressures, both chamber i and upstream chambers can be filled without closing downstream valves.

2) Example for a Series of Binary Actuators: Consider a series of three binary actuators that are either at ambient pressure (0) or inflated (1), see Fig. 2. There are $2^3 = 8$ different states, and since there are only two different pressure levels, there are shortcuts to move between the 8 target pressures. States where chambers far from the source remain unchanged can be reached without going back to the starting configuration (000), see Fig. 2(c).

Since this example has $N = 3$ chambers it requires $N - 1 = 2$ distinctly addressable band-pass valves, Fig. 2(b). In terms of pressure modulation, two such valves require three different pressure settings that result in three different flow speeds through the system: ***slow*** where none of the valves close, ***medium*** where only the sensitive valves furthest from the pressure source close, and ***fast*** where both valves close. Figure 2(c) shows the transition diagram where the three different transitions are labeled. For example, starting from state 000 the three different pressurization speeds result in three different states: 100, 110, or 111.

Note that the separation requirement is between flows of two neighboring band-pass valves and not between the shutoff flows in the two directions of a single band-pass valve. In our physical experiments, Sec. IV, we relax the symmetry assumption to get better separation between actuation pressures in the physical device. However, the above strategy still applies directly.

III. Valve Design

The device described in this section is a prototype design for demonstrating how pressure configurations in a multi-chamber system can be set by modulating the pressure profile from a single source, see Sec. IV. The valve has no active components and the internal parts that determine the operational characteristics can be easily swapped to facilitate exploration of the parameter space. We were able to find enough combinations to implement two independently addressable band-pass valves (and a fifth valve that allows us to disconnect the pressure source), see Fig. 2. We kept the internal geometry relatively simple to facilitate the future development of completely soft and/or miniaturized versions.

A. Physical Design

Our leaky check valve consists of three main functional features contained in a 3D-printed housing: an acrylic orifice plate, a plastic separator to induce leaking, and a rubber flap. There are three operating regimes. In the forward direction, flow deforms the rubber flap, but there are no features for it to seal against. In the backward direction, under low flow conditions, the deflection of the rubber flap is not sufficient to cause it to seal against the orifice plate. However, under high flow conditions, the rubber flap deforms and seals against the orifice plate. Once the flow is shut off, differential pressure across the valve maintains the seal, see Fig. 3(a). The three internal components of a valve are shown in Fig. 3(b).

The 3D-printed housing has two halves that are attached with screws so that the internal components can be quickly and easily exchanged. Grooves in the valve body hold two O-rings: one underneath the orifice plate to prevent air from leaking past the valve and another sealing the two halves of the housing, see Fig. 3(c). The orifice plate, spacer, and valve flap are laser cut from their respective stock materials: 3 mm acrylic, 0.13 mm (5 mil) PET film, and natural latex rubber sheets, durometer 40A, of various thicknesses. The outer diameter of these parts is, 14.5 mm, and the inner diameter for the spacer and flap are 7.5 mm and 9.5 mm respectively. The width of the flap is 5.5 mm, see Fig. 3(b).

B. Device Characterization

We characterized the shutoff pressure for various parameter combinations by connecting the device to a hand operated syringe pump while recording pressure profiles, see Fig. 4. During the test the syringe was connected to the output port of the valve, so that the syringe could be freely filled. Pushing air back out, we moved the plunger at a steadily increasing speed until the pressure reached several psi. The increasing flow rate increases the pressure across the valve, see Fig. 1(b). When the pressure is below $\Delta P_{\text{shutoff}}$, air is vented through the input port. However, once the shutoff pressure is reached, the venting stops and the plunger movement causes compression and a rapid rise in the measured pressure. For each valve combination we repeated this process multiple times to assess repeatability of a particular valve and to get better estimates of the shutoff pressure.

The table in Fig. 5 shows some of the working parameter combinations and the measured shutoff values. As one would expect, thicker (and as a result stiffer) valve flaps resulted in higher shutoff pressures. The values in each row increase

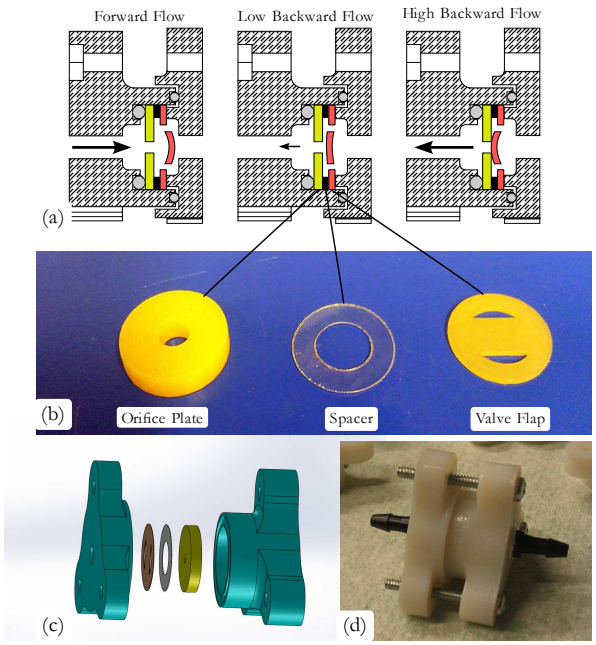

Fig. 3. Picture of valve. (a) Diagram of operational principle. The housing, shown as a hashed cross-section, holds the orifice plate (yellow), spacer (black), and valve flap (red). All forward flow is unimpeded. Low backward flow does not cause sufficient deformation in the valve flap to create a seal. High backward flow seals the valve flap against the orifice plate. The locations of the two internal O-rings are sown in gray. (b) Three different internal components that determine the shutoff pressure: orifice plate, spacer, and valve flap. (c) Exploded view of valve assembly, omitting O-rings and screws. (d) Picture of assembled valve.

monotonically. The relation of the shutoff pressure to the orifice size is more complicated as several factors seem to compete at these size and pressure scales. On the one hand, a larger orifice size decreases the flow resistance, R, allowing more flow at a given pressure. Since moving air has to change momentum to flow around the valve flap, the increased flow should result in a greater deflection and thus a lower shut off pressure. On the other hand, larger holes are more difficult to seal and we suspect that the low shutoff pressures for the 1.5 mm orifices are due to the fact that the smaller holes were easier to close.

There are many opportunities for further characterizing and optimizing of this type of valve. However, an exhaustive design optimization is beyond the scope of this work. Since the goal here is the demonstration of a novel actuation strategy, we focused on identifying a set of valves with sufficiently different shutoff pressures to perform the experiments outlined in the next section.

In addition to the data using 0.13 mm (6 mil) spacers, presented in Fig. 5, we also tested configurations with 0.05 mm (2 mil) spacers and 0.25 mm (10 mil) spacers. For the thinner spacer, some configurations acted like a regular check valves and closed immediately ($\Delta P_{\text{shutoff}} = 0$). For the thicker spacer, some configurations never closed with the pressure differentials we were able to generate ($\Delta P_{\text{shutoff}} > \approx 5$ psi).

IV. Experimental Results

By using several of the valves described in the previous section, we were able to create band-pass valves and reach

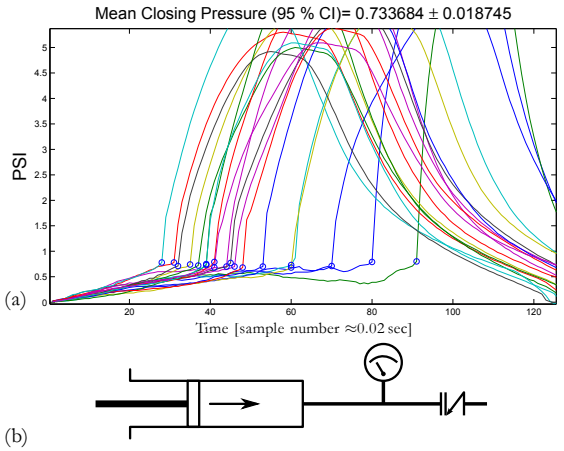

Fig. 4. (a) Pressure trajectories for characterizing shutoff pressure. Each colored trace represents a different trial. (b) The test setup consisted of a large syringe connected to a data-logging pressure sensor and the valve to be characterized. When generating a steadily increasing pressure profile the valve closes and the measured pressure suddenly increases. The pressure at which this kink occurs was estimated by looking for sudden changes in the derivative (blue circles). Each valve was repeatedly closed to get an estimate of the mean and the repeatability of a particular valve.

	Valve Flap Thickness in mm				
Orifice ⌀	0.15	0.30	0.36	0.50	0.76
1.5 mm	**0.037**	0.21	0.57	0.83	3.16
2.0 mm	0.069	0.35	0.64	1.71	2.37
2.5 mm	X	**0.19**	0.44	**0.73**	**1.21**
3.0 mm	X	0.11	0.32	0.39	1.45
3.5 mm	X	0.21	0.31	0.32	1.22

Fig. 5. Shutoff pressures (psi) for different parameter combinations. Each column represents a different thickness flap and each row represents a different orifice size. The spacer in all these configurations is 0.13 mm (5 mil). The X's indicate combinations were the valve flap burst during operation. Bold entries correspond to valve parameters used in the experiments.

stable pressure configurations with three pneumatic soft-robotic actuators that act as pressure chambers, see Fig. 6. The valves that connect them are completely passive, and the only controlled input is a hand-operated syringe pump.

Asymmetric pass-bands resulted in good shutoff pressure separation in both the pressurizing and depressurizing direction. The smaller orifices in the second band-pass valve compared to the first also resulted in better pass-band separation according to Eqn. (5). The separation was large enough to allow reliable manual operation.

We performed a depth-first traversal of the configuration tree shown in Fig. 2 starting in configuration 000 and exploring the branches top to bottom. Figure 7 shows the measured pressures of all three actuators and the input pressure as a function of time. The single modulated pressure source was sufficient to reach all eight configurations. The 15 states that had to be visited for a complete traversal are highlighted above and below the pressure traces.

The beginning of the traces shows that the pressure source can be disconnected while the network maintains its pressure configuration. The pressure P_1 is high ($P_1 = 1$), while P_{in} is low ($P_{\text{in}} = 0$), see Fig. 7(b). The slow transitions to go between states 000 and 111 are particularly clear in the pressure traces, see Fig. 7(g)–(h) and (n)–(o).

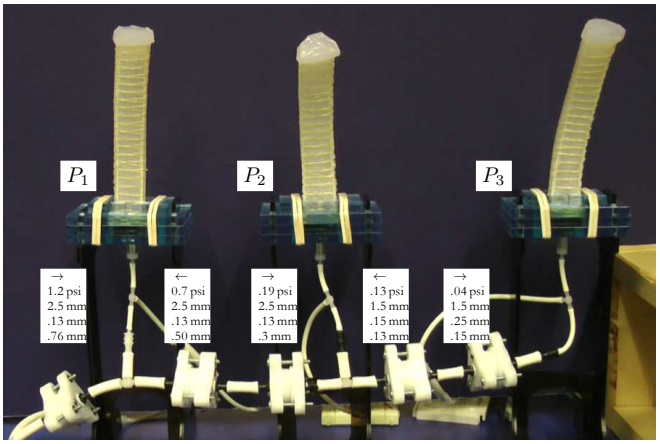

Fig. 6. Photo of experimental setup showing three soft-robotic pneumatic actuators and five valves, see Fig. 2. The pressure source is to the left of the picture. The thin white pressure lines that fork off the actuator supply lines are connected to digital pressure sensors. The white boxes show the parameters of the valve below: direction, shutoff pressure, orifice diameters, spacer thickness, and flap thickness.

Low shutoff pressures and flows limit the actuation speed, and the number of chambers is limited by the required separation between the shutoff pressures/flows. The separation must obey the restrictions given in Eqn. (4) and (5) and additionally account for limits on the modulation accuracy of the pressure source. Thus overall system performance can be improved by designing better pressure sources with finer pressure control, improving valve manufacturing with more precise shutoff pressures, and employing higher operating pressures that can accommodate more pass-bands.

We focused on binary pressure combinations, but intermediate pressure levels should be equally easy to achieve with a similar strategy. Also, we focused on a simple serial connection, but for some robotic or microfluidic applications parallel arrangements could be advantageous. The presented band-pass valve design control strategy could easily be adapted to such new scenarios.

V. Conclusion and Future Work

We presented an idealized valve model and a control strategy that allows filling multiple connected chambers to different pressure levels. The operational theory of this valve is to deliberately introduce a gap to allow backward flow into a check valve design. Connecting two of these valves in series results in a band-pass valve, which can be used to selectively gate different chambers from being filled/drained. The simple design should allow this type of valve to be implemented with different materials and at different length scales. We demonstrate the approach with serially connected soft-robotic actuators and a prototype valve design on a cm-scale. The main limitation of our approach is that filling pressures need to be controlled more accurately than filling single pressure chambers, and that it introduces dependencies between state variables: at a given time possible filling rates for a given chamber depend both on the connection topology of chambers and their pressure states.

For both soft-robotic and microfluidic applications, the immediate next step is to design valves that can be incorporated in the existing manufacturing processes. Since the key functional component is a flexible flap with carefully controlled

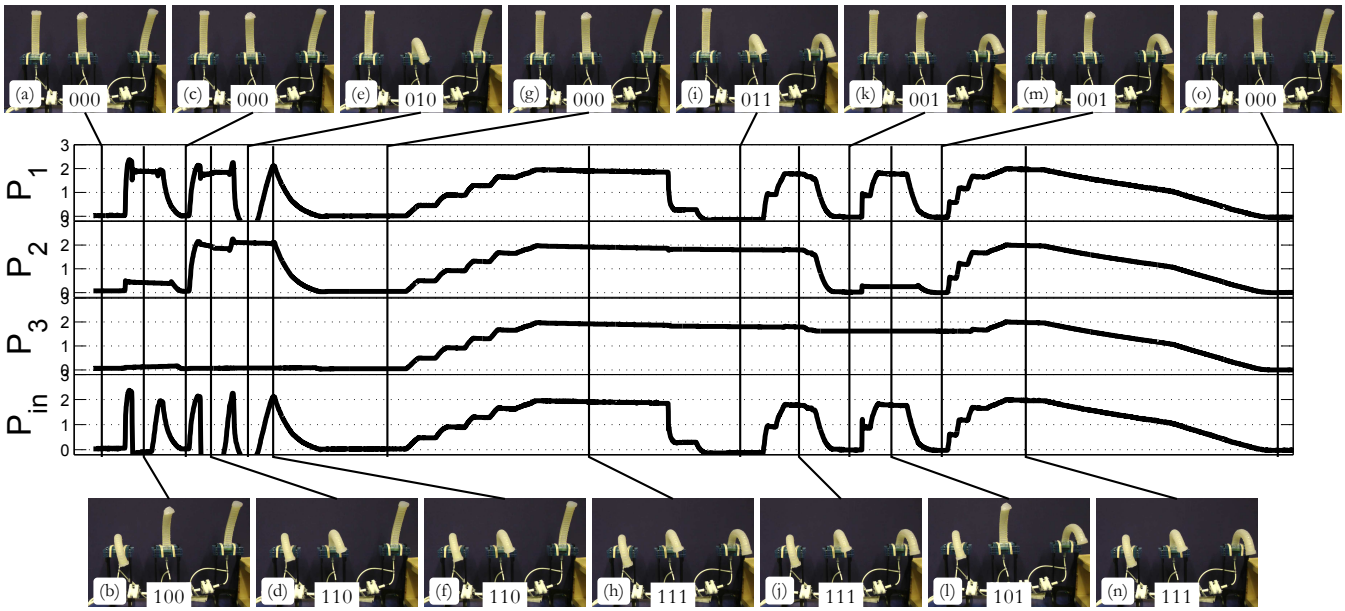

Fig. 7. Pressure profile of input pressure (bottom) and the pressures P_1, P_2, P_3 in the three connected chambers. The chambers reach all possible binary (hihgh/low pressure) combinations via a depth-first traversal of the configuration tree, Fig. 2(c). The 15 states along the traversal are marked in time by vertical lines and shown above and blow the traces as video frames.

thickness and spacing, we expect that incorporating it into soft lithography (microfluidics) and casting (soft robots) is possible. This would allow producing less expensive robots with fewer complex components and microfluidic chips with fewer external pressure lines.

By more carefully modeling and characterizing these band-pass valves we expect much more aggressive control strategies to be possible. The models presented here are idealized linear versions, and we ignore pressure losses along connecting lines. Especially in microfluidic applications where the chamber volumes are small and the routing lines comparatively long, creating more complete models would likely improve the reliability of operating many addressable pressure chambers from a single supply line. Similarly, we chose a serial network topology because it results in a simple control strategy, but parallel connections or mixtures of the two are possible and might simplify actuation for specific applications or provide robustness to device failures.

Acknowledgements

We would like to thank Dr. Kevin Galloway, Dr. Michael Wehner, and Prof. Robert Wood's Microrobotics lab as a whole. We are grateful for the support of the Wyss Institute at Harvard which made this work possible.

References

[1] Deepak Trivedi, Christopher D Rahn, William M Kier, and Ian D Walker. Soft robotics: Biological inspiration, state of the art, and future research. *Applied Bionics and Biomechanics*, 5(3):99–117, 2008.

[2] Kyu-Jin Cho, Je-Sung Koh, Sangwoo Kim, Won-Shik Chu, Yongtaek Hong, and Sung-Hoon Ahn. Review of manufacturing processes for soft biomimetic robots. *International Journal of Precision Engineering and Manufacturing*, 10(3):171–181, 2009.

[3] Rolf Pfeifer, Max Lungarella, and Fumiya Iida. The challenges ahead for bio-inspired 'soft' robotics. *Communications of the ACM*, 55(11):76–87, 2012.

[4] Carmel Majidi. Soft robotics: A perspectivecurrent trends and prospects for the future. *Soft Robotics*, 1(P):5–11, 2013.

[5] Filip Ilievski, Aaron D Mazzeo, Robert F Shepherd, Xin Chen, and George M Whitesides. Soft robotics for chemists. *Angewandte Chemie*, 123(8):1930–1935, 2011.

[6] Robert F Shepherd, Filip Ilievski, Wonjae Choi, Stephen A Morin, Adam A Stokes, Aaron D Mazzeo, Xin Chen, Michael Wang, and George M Whitesides. Multigait soft robot. *Proceedings of the National Academy of Sciences*, 108(51):20400–20403, 2011.

[7] SM Spearing. Materials issues in microelectromechanical systems (mems). *Acta Materialia*, 48(1):179–196, 2000.

[8] William McMahan, V Chitrakaran, M Csencsits, D Dawson, Ian D Walker, Bryan A Jones, M Pritts, D Dienno, M Grissom, and Christopher D Rahn. Field trials and testing of the octarm continuum manipulator. In *Robotics and Automation (ICRA), 2006 IEEE International Conference on*, pages 2336–2341. IEEE, 2006.

[9] Cagdas D. Onal, ' '1 2'Xin Chen, George M. Whitesides, and Daniela Rus. Soft mobile robots with on-board chemical pressure generation. In *15th International Symposium on Robotics Research Flagstaff, AZ 28 August - 1 September*, 2011.

[10] Andrew D. Marchese, C.D. Onal, and D. Rus. Soft robot actuators using energy-efficient valves controlled by electropermanent magnets. In *Intelligent Robots and Systems (IROS), 2011 IEEE/RSJ International Conference on*, pages 756–761, 2011.

[11] Y. Nishioka, K. Suzumori, T. Kanda, and S. Wakimoto. Experimental evaluation of multiplex penumatic control drive. In *World Automation Congress (WAC), 2010*, pages 1–6, 2010.

[12] Robert F. Shepherd, Adam A. Stokes, Jacob Freake, Jabulani Barber, Phillip W. Snyder, Aaron D. Mazzeo, Ludovico Cademartiri, Stephen A. Morin, and George M. Whitesides. Using explosions to power a soft robot. *Angewandte Chemie International Edition*, 52(10):2892–2896, 2013.

[13] George M Whitesides. The origins and the future of microfluidics. *Nature*, 442(7101):368–373, 2006.

[14] Marc A. Unger, Hou-Pu Chou, Todd Thorsen, Axel Scherer, and Stephen R. Quake. Monolithic microfabricated valves and pumps by multilayer soft lithography. *Science*, 288(5463):113–116, 2000.

[15] William H. Grover, Robin H. C. Ivester, Erik C. Jensen, and Richard A. Mathies. Development and multiplexed control of latching pneumatic valves using microfluidic logical structures. *Lab Chip*, 6:623–631, 2006.

[16] James A Weaver, Jessica Melin, Don Stark, Stephen R Quake, and Mark A Horowitz. Static control logic for microfluidic devices using pressure-gain valves. *Nature Physics*, 6(3):218–223, 2010.

[17] Naga Sai Gopi K. Devaraju and Marc A. Unger. Pressure driven digital logic in pdms based microfluidic devices fabricated by multilayer soft lithography. *Lab Chip*, 12:4809–4815, 2012.